

Porous Tungsten Carbide Nanoplates Derived from Tungsten Trioxide Nanoplates

Deliang Chen,^{‡,†} Haitao Zhai,[‡] Huimin Chen,[§] Yi Zhang,[‡] Bingbing Fan,[‡] Hailong Wang,[‡] Hongxia Lu,[‡] Zhengxin Li,^{‡,¶} Rui Zhang,^{‡,||} Jing Sun,^{††} and Lian Gao^{††}

[‡]School of Materials Science and Engineering, Zhengzhou University, 100 Science Road, Zhengzhou 450001, China

[§]China Academy of Launch Vehicle Technology, 1 South Dahongmen, Beijing 100076, China

[¶]School of Materials Science and Engineering, Henan University of Technology, 195 Zhongyuan West Road, Zhengzhou 450007, China

^{||}Laboratory of Aeronautical Composites, Zhengzhou Institute of Aeronautical Industry Management, Zhengzhou 450046, China

^{††}The State Key Laboratory of High Performance Ceramics and Superfine Microstructure, Shanghai Institute of Ceramics, Chinese Academy of Sciences, 1295 Dingxi Road, Shanghai 200050, China

Porous WC nanoplates (PWCPs) were synthesized by a nitridization-carbonization process using WO₃ nanoplates as the precursor for morphological control. The WO₃ nanoplates were derived from tungstate-based inorganic-organic hybrid belts. The synthesis of PWCPs involved a nitridization reaction of WO₃ nanoplates in NH₃ at 650°C for 2 h, followed by a carbonization reaction in a CO/CO₂ (10:1, v/v) mixture at 750°C for 10 h. The as-obtained product is a pure hexagonal WC phase with a plate-like and porous morphology. The aggregates of the PWCPs with dimensions of (100–300) × (10–30) nm form a house-of-card structure with open channels and high-specific surface areas, and can act as potential supports of electrocatalysts for high-performance fuel cells.

I. Introduction

TUNGSTEN carbide (WC) nanostructures and their nanocomposites have attracted increasing attention in electrocatalytical applications for fuel cells due to their Pt-like electrical structure and their synergistic effect with other metal clusters.^{1–3} For electrocatalytical applications, high surface areas and good dispersibility are essential requirements. To achieve this purpose, many groups have developed various methods to prepare nanoscale WC nanocrystals, including WC nanoparticles on support,^{4–6} free-standing WC nanoparticles,^{7,8} mesoporous WC nanochains,⁹ WC nanofibers,¹⁰ WC nanorods and nanopatelets,¹¹ hollow WC microspheres,¹² three-dimensionally ordered macroporous WC,¹³ hierarchical WC micro/nanocrystals,¹⁴ and inverse opal WC nanostructures.¹⁵ However, morphology-controlled synthesis of low-dimensional tungsten carbide nanostructures (e.g., nanoplates) with high surface areas and high redispersibility is still a harsh challenge.

We here introduce an efficient approach to synthesize porous WC nanoplates (PWCPs) with large diameter-to-thickness

ratios and high specific surface areas on the basis of topochemical conversion and intercalation chemistry.^{16–18} Essentially, the PWCPs are synthesized via a two-step nitridization-carbonization method using two-dimensional WO₃ nanoplates as intermediates for morphological control. This method is cost-effective, easy to control, and suitable for large-scale production.

II. Experimental Procedure

The WO₃ nanoplates were synthesized according to our previous report.¹⁷ Typically, H₂W₂O₇·xH₂O (~5 g) was dispersed in a mixture of *n*-octylamine (~33 mL) and heptane (160 mL) under magnetic stirring, and kept reacting for 3 d. After the reaction, a white solid, i.e., the THBs, was collected and dried. The as-obtained THBs (~5 g) were dispersed in a HNO₃ aqueous solution (~6 mol/L, 150 mL) and kept stirring for 2 d at room temperature. The solid was collected, washed, and dried at 120°C. The yellow powders obtained, H₂WO₄ nanoplates, were calcined at 400°C for 2 h in air to synthesize WO₃ nanoplates.

The WO₃ nanoplates (~0.5 g) were uniformly covered on the surface of a rectangular Al₂O₃ plate (128 mm × 29 mm × 4 mm), which was then horizontally put in a semicylindrical Al₂O₃ boat (φ 42 mm × 29 mm × 5 mm). The boat with WO₃ nanoplates was carefully pushed to the center of a quartz tube (φ 46 mm × 600 mm) of a horizontal tubular furnace. After sealing carefully, the furnace was firstly purged with CO₂ gas (100 mL/min) for 20 min to discharge the residual air. Then, the CO₂ gas was switched to NH₃ gas (100 mL/min), and the furnace was heated to 500°C with a rate of 25°C/min, and then to 650°C with a rate of 10°C/min. The nitridization reaction was kept for 2 h at 650°C. The NH₃ gas was then changed to a CO/CO₂ mixture (100 mL/min, V_{CO}:V_{CO2} = 10:1) and the temperature was increased to 750°C (heating rate: 10°C/min), at which the carbonization reaction was kept for another 10 h. Finally, the sample (e.g., PWCPs) was cooled and collected for characterization.

XRD (CuKα; ZHJ XPRT PRO, China), SEM (JEOM-6700F, Japan), TEM (200 kV; Tecnai-G20), N₂ adsorption-desorption (Nova 4200a), TG-DTA (Netzsch STA409PC, Germany), and FT-IR (Nicolet460) were used to characterize the as-obtained PWCPs and their precursors.

J. Yu—contributing editor

III. Results and Discussion

Figure 1(a) shows an XRD pattern of the WO_3 nanoplates obtained from a tungstate-based inorganic-organic hybrid compound, formed via acid-base reactions between $\text{H}_2\text{W}_2\text{O}_7 \cdot x\text{H}_2\text{O}$ and *n*-octylamine.¹⁸ As the XRD pattern in the inset of Fig. 1(a) shows, the hybrid has a series of peaks located in the low 2θ range (less than 25°), and the peaks are attributable to (00 l) reflections, characteristic of a highly-ordered lamellar structure with an interlayer distance of 2.597(2) nm.¹⁸ As the SEM image in Fig. 2(a) shows, the as-obtained hybrid consists of a one-dimensional belt-like structure, being 10–50 μm long and 0.5–1 μm in apparent diameter. The TG-DTA and FT-IR analyses (not shown) indicated that the belts are of an inorganic-organic hybrid lamellar structure, alternately stacking inorganic W–O layers and organic amine layers.¹⁸ The WO_3 nanoplates were synthesized by selectively removing the organic species from the hybrid belts.¹⁷ The as-obtained WO_3 nanoplates are indexed to a monoclinic WO_3 phase (JCPDS no. 43-1035) according to the XRD pattern [Fig. 1(a)]. Figure 2(b) shows a SEM image of the as-obtained WO_3 nanoplates, which is loosely assembled to form a house-of-card structure with high surface areas.¹⁷

The WC sample (PWCPs) derived from the as-obtained WO_3 nanoplates shows three strongest peaks located at 31.4° , 35.6° , and 48.3° in its XRD pattern [Fig. 1(b)], being indexed to (001), (100), and (101) reflections of a hexagonal WC phase (JCPDS no. 25-1047, $a = 2.9062$ and $c = 2.8378$ Å), respectively. Other weak peaks (not shown) in the XRD pattern are also in good agreement with the hexagonal WC phase, and no peaks belong to impurities. The calculated cell parameters [$a = 2.896(3)$ and $c = 2.847(8)$ Å] are close to the literature data. The SEM image in Fig. 2(c) shows that the WC sample consists of uniform plate-like particles, similar to their precursor of WO_3 nanoplates [Fig. 2(b)]. The high-magnification SEM image in Fig. 2(d) indicates that the WC nanoplates, with dimensions of 200–500 nm in areas and 10–30 nm in thicknesses, are of pores with various sizes.

Figure 3 shows the TEM observations of the porous WC nanoplates (PWCPs). A low-magnification TEM image in Fig. 3(a) confirms that a WC nanoplate consists of small particles overlapped on one another, forming a quasi two-dimensional and porous morphology. The corresponding high-magnification TEM image [Fig. 3(b)] indicates that the PWCPs consist of interconnected nanoparticles with a size range of 10–20 nm. A high-resolution TEM image in

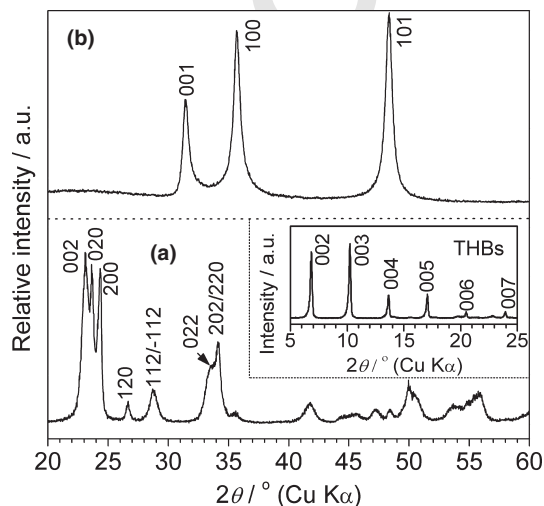


Fig. 1. (a) XRD pattern of the WO_3 nanoplates derived from the tungstate-based inorganic-organic hybrid belts (THBs); (b) XRD pattern of the porous WC nanoplates (PWCPs) derived from the WO_3 nanoplates. The inset is the XRD pattern of the (THBs).

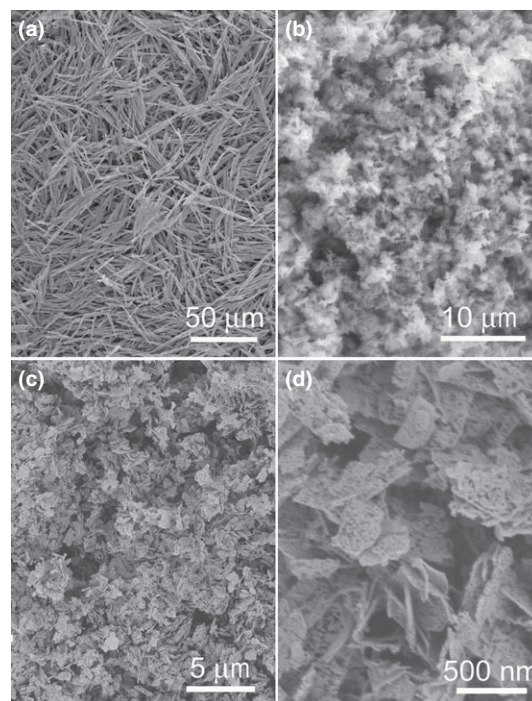


Fig. 2. SEM images of (a) the tungstate-based inorganic-organic hybrid belts (THBs) and the corresponding (b) WO_3 nanoplates and (c–d) porous WC nanoplates (PWCPs) derived from the THBs.

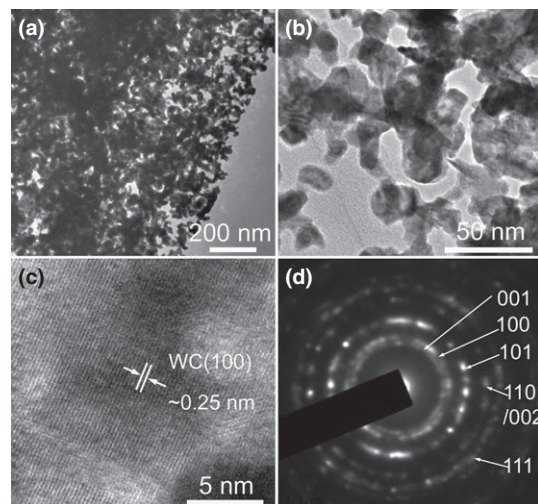


Fig. 3. (a–b) TEM images, (c) HR-TEM image, and (d) SAED pattern of the porous WC nanoplates derived from the tungstate-based hybrid belts.

Fig. 3(c) shows ordered lattice fringes with a lattice spacing of ~ 0.25 nm, attributable to the (100) planes of hexagonal WC phase. The corresponding SAED pattern in Fig. 3(d) shows a series of discontinuous diffraction rings belonging to hexagonal WC phase. The elements of the sample determined by EDS spectra are W and C. The TG-DTA curves (not shown) of the PWCPs had a mass gain of 12.4% and exothermic peak at 420°C – 486°C , mainly due to the oxidation of WC, besides a small amount of residual carbon. The mass fraction of the residual carbon was calculated to be ~ 4.5 wt% according to the TG-DTA analysis.

Figure 4 shows the N_2 adsorption-desorption isotherm curves and pore-size distribution of the as-obtained PWCPs. The N_2 adsorption-desorption isotherm is of type IV, and the high absorption at high relative pressure (P/P_0) range (approaching 1.0) suggests the formation of large mesopores

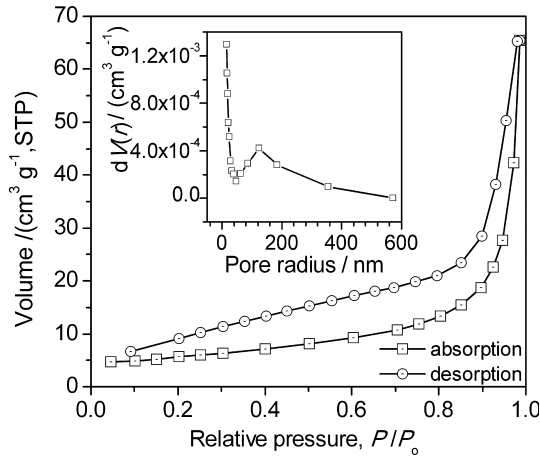
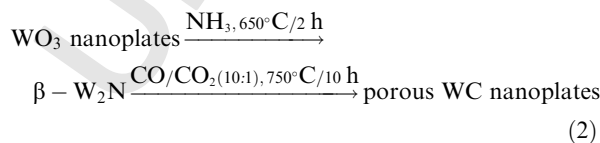
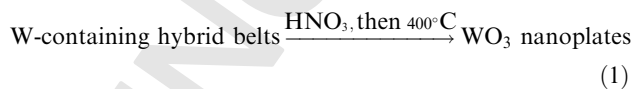


Fig. 4. Nitrogen adsorption-desorption isotherm curves and the pore-size distribution based on the BJH method adsorption (the inset) of the porous WC nanoplates derived from the tungstate-based hybrid belts.

(2–50 nm) and macropores (>50 nm) in the PWCPs sample.^{19–21} The shape of hysteresis loops is of type H3, associated with aggregates of plate-like particles, giving rise to slit-like pores.²¹ The low-pressure hysteresis also indicates that the PWCPs contain some micropores (<2 nm).²¹ Actually, the pore-size distribution (the inset of Fig. 4) confirms that there are three types of pores: macropores (50 < φ < 500 nm), micropores, and mesopores (φ < 50 nm).²¹ The micropores and mesopores mainly are due to the in-plane pores of an individual WC nanoplate [Figs. 3(a)–(b)], whereas the macropores are mainly caused by the house-of-card structure of the aggregated PWCPs [Fig. 2(d)]. The specific surface area of the PWCPs is 19.5 m²/g according to the multipoint BET plot.

The formation of the PWCPs may involve the essential reactions as shown in Eqs. 1–2.^{8,16–18} The plate-like shape is inherited from the WO₃ nanoplates to WC nanoplates via a tungsten nitride.¹⁶ The formation mechanism of the micropores and mesopores in PWCPs can be understood from the following aspects: (1) the shrinkage in volume during the conversion from monoclinic WO₃ (7.2 g/cm³) to β-W₂N, and then to hexagonal WC (15.6 g/cm³) due to the difference in density and (2) the framework support effect of the solid plate-like morphology which prevent the mass transfer during the nitridization and carbonization reactions. The synergistic effect of the shrinkage in volume and the steric hindrance of plate-like morphology in mass transfer facilitate the formation of porous WC nanoplates from WO₃ nanoplates.^{8,16}



The carbonization temperature and CO₂/CO ratios have important effects on the formation of pure WC phase, and low temperature (<750°C) or high CO₂/CO ratios (>10:1) are unfavorable in the synthesis of WC. The subprocess of nitridization plays a key role in the formation of porous morphology by refining the grains of WC phase.^{8,16} The plate-like shape of the WO₃ precursor is necessary for the

formation of WC nanoplates via a topochemical conversion, and the precursors with other morphologies are not easy to produce porous WC nanoplates.^{8,11,14}

IV. Conclusions

Porous WC nanoplates with high surface areas have been synthesized for the first time by a topochemical conversion process, involving a nitridization reaction at 650°C in NH₃ and a carbonization reaction at 750°C in a mixture of CO/CO₂. The WC nanoplates obtained have in-plane micropores, mesopores (<50 nm), and macropores from their aggregates with a house-of-card structure. The porous WC nanoplates can be used as potential supports for high-performance electrocatalysts.

Acknowledgments

This work was supported by the National Natural Science Foundation of China (no. 51172211 and 50802090), the China Postdoctoral Science Foundation (no. 201003397), the Foundation for University Young Key Teacher by Henan Province (no. 2011GGJS-001), and the Advanced Programs of Returned Overseas Researchers of Henan Province (no. [2011] 17).

References

- Z. J. Mellinger, T. G. Kelly, and J. G. Chen, "Pd-Modified Tungsten Carbide for Methanol Electro-Oxidation: From Surface Science Studies to Electrochemical Evaluation," *ACS Catal.*, **2** [5] 751–8 (2012).
- S. Yin, M. Cai, C. Wang, and P. K. Shen, "Tungsten Carbide Promoted Pd-Fe as Alcohol-Tolerant Electrocatalysts for Oxygen Reduction Reactions," *Energy Environ. Sci.*, **4** [2] 558–63 (2011).
- A. L. Stottlemeyer, E. C. Weigert, and J. G. Chen, "Tungsten Carbides as Alternative Electrocatalysts: From Surface Science Studies to Fuel Cell Evaluation," *Ind. Eng. Chem. Res.*, **50** [1] 16–22 (2011).
- J. L. Lu, Z. H. Li, S. P. Jiang, P. K. Shen, and L. Li, "Nanostructured Tungsten Carbide/Carbon Composites Synthesized by a Microwave Heating Method as Supports of Platinum Catalysts for Methanol Oxidation," *J. Power Sources*, **202**, 56–62 (2012).
- Z. Yan, H. Meng, P. K. Shen, R. Wang, L. Wang, K. Shi, and H. Fu, "A Facile Route to Carbide-Based Electrocatalytic Nanocomposites," *J. Mater. Chem.*, **22** [11] 5072–9 (2012).
- G. He, Z. Yan, X. Ma, H. Meng, P. K. Shen, and C. Wang, "A Universal Method to Synthesize Nanoscale Carbides as Electrocatalyst Supports Towards Oxygen Reduction Reaction," *Nanoscale*, **3** [9] 3578–82 (2011).
- T. G. Ryu, H. Y. Sohn, K. S. Hwang, and Z. Z. G. Fang, "Plasma Synthesis of Tungsten Carbide Nanopowder From Ammonium Paratungstate," *J. Am. Ceram. Soc.*, **92** [3] 655–60 (2009).
- S.-K. Sun, Y.-M. Kan, G.-J. Zhang, and P.-L. Wang, "Ultra-Fine Tungsten Carbide Powder Prepared by a Nitridation-Carbonization Method," *J. Am. Ceram. Soc.*, **93** [11] 3565–8 (2010).
- Y. Wang, S. Q. Song, P. K. Shen, C. X. Guo, and C. M. Li, "Nanochain-Structured Mesoporous Tungsten Carbide and Its Superior Electrocatalysis," *J. Mater. Chem.*, **19** [34] 6149–53 (2009).
- X. Zhou, Y. Qiu, J. Yu, J. Yin, and S. Gao, "Tungsten Carbide Nanofibers Prepared by Electrospinning With High Electrocatalytic Activity for Oxygen Reduction," *Int. J. Hydrogen Energy*, **36** [13] 7398–404 (2011).
- S. Shanmugam, D. S. Jacob, and A. Gedanken, "Solid State Synthesis of Tungsten Carbide Nanorods and Nanoplatelets by a Single-Step Pyrolysis," *J. Phys. Chem. B*, **109** [41] 19056–9 (2005).
- J. B. d'Arbigny, G. Taillades, M. Marrony, D. J. Jones, and J. Rozière, "Hollow Microspheres With a Tungsten Carbide Kernel for PEMFC Application," *Chem. Commun.*, **47** [28] 7950–2 (2011).
- J. P. Bosco, K. Sasaki, M. Sadakane, W. Ueda, and J. G. G. Chen, "Synthesis and Characterization of Three-Dimensionally Ordered Macroporous (3DOM) Tungsten Carbide: Application to Direct Methanol Fuel Cells," *Chem. Mater.*, **22** [3] 966–73 (2010).
- D. Chen, H. Wen, H. Zhai, H. Wang, X. Li, R. Zhang, J. Sun, and L. Gao, "Novel Synthesis of Hierarchical Tungsten Carbide Micro-/Nanocrystals From a Single-Source Precursor," *J. Am. Ceram. Soc.*, **93** [12] 3997–4000 (2010).
- J. C. Lyle, N. R. Denny, R. T. Turgeon, and A. Stein, "Pseudomorphic Transformation of Inverse Opal Tungsten Oxide to Tungsten Carbide," *Adv. Mater.*, **19** [21] 3682–6 (2007).
- D. Chen, H. Wen, T. Li, L. Yin, B. Fan, H. Wang, R. Zhang, X. Li, H. Xu, H. Lu, D. Yang, J. Sun, and L. Gao, "Novel Pseudo-Morphotactic Synthesis and Characterization of Tungsten Nitride Nanoplates," *J. Solid State Chem.*, **184** [2] 455–62 (2011).
- D. Chen, L. Gao, A. Yasumori, K. Kuroda, and Y. Sugahara, "Size- and Shape-Controlled Conversion of Tungstate-Based Inorganic-Organic Hybrid Belts to WO₃ Nanoplates With High Specific Surface Areas," *Small*, **4** [10] 1813–22 (2008).
- D. Chen, and Y. Sugahara, "Tungstate-Based Inorganic-Organic Hybrid Nanobelts/Nanotubes With Lamellar Mesostructures: Synthesis, Characterization, and Formation Mechanism," *Chem. Mater.*, **19** [7] 1808–15 (2007).

1 ¹⁹J. Zhang, J. Yu, Y. Zhang, Q. Li, and J. R. Gong, "Visible Light
2 Photocatalytic H₂-Production Activity of CuS/ZnS Porous Nanosheets Based
3 on Photoinduced Interfacial Charge Transfer," *Nano Lett.*, **11** [11] 4774–9
4 (2011).

5 ²⁰W. Cai, J. Yu, B. Cheng, B.-L. Su, and M. Jaroniec, "Synthesis of Boehm-
6 ite Hollow Core/Shell and Hollow Microspheres via Sodium Tartrate-Medi-

ated Phase Transformation and Their Enhanced Adsorption Performance in
Water Treatment," *J. Phys. Chem. C*, **113** [33] 14739–46 (2009).

7 ²¹K. S. W. Sing, D. H. Everett, R. A. W. Haul, L. Moscou, R. A. Pierotti,
8 J. Rouquerol, and T. Siemieniewska, "Physical and Biophysical Chemistry
9 Division Commission on Colloid and Surface Chemistry Including Catalysis,"
10 *Pure Appl. Chem.*, **57** [4] 603–19 (1985). □

11
12
13
14
15
16
17
18
19
20
21
22
23
24
25
26
27
28
29
30
31
32
33
34
35
36
37
38
39
40
41
42
43
44
45
46
47
48
49
50
51
52
53
54
55
56
57
58
59
60
61
62
63
64
65
66
67
68
69
70
71
72

Author Query Form

Journal: JACE
Article: 5449

Dear Author,

During the copy-editing of your paper, the following queries arose. Please respond to these by marking up your proofs with the necessary changes/additions. Please write your answers on the query sheet if there is insufficient space on the page proofs. Please write clearly and follow the conventions shown on the attached corrections sheet. If returning the proof by fax do not write too close to the paper's edge. Please remember that illegible mark-ups may delay publication.

Many thanks for your assistance.

Query reference	Query	Remarks
1	AUTHOR: Please check that the title, author names, affiliations, and corresponding author information is listed accurately for publication.	
2	AUTHOR: Please provide city information for CuKα; ZHJ XPERT PRO, China	
3	AUTHOR: Please give manufacturer information for JEOM-6700F, Japan: company name, town, state (if USA), and country.	
4	AUTHOR: Please give manufacturer information for Tecnai-G20: company name, town, state (if USA), and country.	
5	AUTHOR: Please give manufacturer information for Nova 4200a: company name, town, state.	
6	AUTHOR: Please give manufacturer information for Netzsch STA409PC, Germany: company name, town, state (if USA), and country.	
7	AUTHOR: Please give manufacturer information for Nicolet460: company name, town, state (if USA), and country.	

Proof Correction Marks

Please correct and return your proofs using the proof correction marks below. For a more detailed look at using these marks please reference the most recent edition of The Chicago Manual of Style and visit them on the Web at: <http://www.chicagomanualofstyle.org/home.html>

<i>Instruction to typesetter</i>	<i>Textual mark</i>	<i>Marginal mark</i>
Leave unchanged	... under matter to remain	<u>stet</u>
Insert in text the matter indicated in the margin	^	^ followed by new matter
Delete	Ʒ through single character, rule or underline or Ʒ through all characters to be deleted	Ʒ
Substitute character or substitute part of one or more word(s)	Ƶ through letter or — through characters	new character Ƶ or new characters Ƶ
Change to italics	— under matter to be changed	<u>ital</u>
Change to capitals	≡ under matter to be changed	<u>Caps</u>
Change to small capitals	≡ under matter to be changed	<u>sc</u>
Change to bold type	~ under matter to be changed	<u>bf</u>
Change to bold italic	~ under matter to be changed	<u>bf+ital</u>
Change to lower case	Ɔ	<u>lc</u>
Insert superscript	√	√ under character e.g. √
Insert subscript	^	^ over character e.g. ^
Insert full stop	⊙	⊙
Insert comma	↕	↕
Insert single quotation marks	↙ ↘	↙ ↘
Insert double quotation marks	↗ ↖	↗ ↖
Insert hyphen	=	=
Start new paragraph	¶	¶
Transpose	┌┐	┌┐
Close up	linking ○ characters	○
Insert or substitute space between characters or words	#	#
Reduce space between characters or words	◌	◌